Intraindividual Comparison of ^{99m}Tc-Methylene Diphosphonate and Prostate-Specific Membrane Antigen Ligand ^{99m}Tc-MIP-1427 in Patients with Osseous Metastasized Prostate Cancer

Hendrik Rathke[1], Ali Afshar-Oromieh[1], Frederik Lars Giesel[1], Christophe Kremer[1], Paul Flechsig[1], Sabine Haufe[1], Walter Mier[1], Tim Holland-Letz[2], Maximilian De Bucourt[3], Thomas Armor[4], John W. Babich[5], Uwe Haberkorn[1,6], and Clemens Kratochwil[1]

[1]Department of Nuclear Medicine, University Hospital Heidelberg, Heidelberg, Germany; [2]Department of Biostatistics, German Cancer Research Center, Heidelberg, Germany; [3]Department of Radiology, Charité-University Medicine, Berlin, Germany; [4]Progenics Pharmaceuticals Inc., New York, New York; [5]Division of Radiopharmaceutical Sciences, Department of Radiology, Weill Cornell Medical College, New York, New York; and [6]Clinical Cooperation Unit Nuclear Medicine, German Cancer Research Center, Heidelberg, Germany

The objective of this study was to evaluate the rate of detection of bone metastases obtained with the prostate-specific membrane antigen (PSMA)–targeting tracer ^{99m}Tc-MIP-1427, as opposed to conventional bone scanning with ^{99m}Tc-methylene diphosphonate (^{99m}Tc-MDP), in a collective of patients with known advanced-stage osseous metastasized prostate cancer. **Methods:** Twenty-one patients with known metastatic disease were staged with both conventional bone scanning and PSMA ligand scintigraphy within a time frame of less than 10 d. Imaging included planar whole-body scanning and SPECT or SPECT/CT with 2 bed positions 3 h after injection of either 500–750 MBq of ^{99m}Tc-MIP-1427 or 600–750 MBq of ^{99m}Tc-MDP. Lesions were scored as typical tumor, equivocal (benign/malignant), or normal within a standard reporting schema divided into defined anatomic regions. Masked and consensus readings were performed with sequential unmasking: planar scans first, then SPECT/CT, the best evaluable comparator (including MRI), PET/CT, and follow-up examinations. **Results:** Eleven patients had PSMA-positive visceral metastases that were predictably not diagnosed with conventional bone scanning. However, SPECT/CT was required to distinguish between soft-tissue uptake and overlapping bone. Four patients had extensive ^{99m}Tc-MDP–negative bone marrow lesions. Seven patients had superscan characteristics on bone scans; in contrast, the extent of red marrow involvement was more evident on PSMA scans. Only 3 patients had equivalent results on bone scans and PSMA scans. In 16 patients, more suspect lesions were detected with PSMA scanning than with bone scanning. In 2 patients (10%), a PSMA-negative tumor phenotype was present. **Conclusion:** PSMA scanning provided a clear advantage over bone scanning by reducing the number of equivocal findings in most patients. SPECT/CT was pivotal for differentiating bone metastases from extraosseous tumor lesions.

Key Words: genitourinary oncology; SPECT; SPECT/CT; intraindividual comparison; PSMA; radioligand; bone scan

J Nucl Med 2018; 59:1373–1379

DOI: 10.2967/jnumed.117.200220

In early-stage prostate cancer, imaging is often performed with curative intent for very low prostate-specific antigen (PSA) levels and very small tumor lesions. In this setting, maximum spatial image resolution and optimal signal-to-noise ratios are important. Prostate-specific membrane antigen (PSMA)–targeting PET/CT is a novel advance that has already demonstrated promising results for primary tumor and lymph node staging as well as for tumor allocation in biochemical relapse (*1–3*). However, PET/CT is not widely available in less developed countries, and the number of γ-cameras worldwide exceeds the number of PET/CT scanners. Consequently, ^{99m}Tc-labeled PSMA tracers have been developed and have already been applied in phase 1 or phase 2 studies (*4–7*)—but predominantly for patients with early-stage prostate cancer, that is, before prostatectomy or in biochemical recurrence. In contrast, conventional bone scanning (BS) is of limited value in early-stage prostate cancer because positive findings are rare until PSA levels increase to greater than 30 ng/mL (*8,9*).

On the other hand, more than 90% of patients with metastatic castration-resistant prostate cancer develop bone involvement over time (*10*). It has already been proven that ^{18}F-NaF PET/CT is superior to conventional ^{99m}Tc-labeled BS for the diagnosis of bone metastasis in prostate cancer and other tumors (*11–13*). However, after curative approaches have been exhausted, improved lesion-level detection rates have limited clinical consequences because patients have already received systemic therapy and the clinical question concerns determining whether there is progression rather than counting lesion numbers. The recent Prostate Cancer Clinical Trials Working Group 3 recommendation suggested that BS is one of the most reliable tools for response assessment (*14*). Thus, BS is still the mainstay for follow-up examinations of metastatic castration-resistant prostate cancer patients given systemic therapy (*15–17*). In

Received Oct. 5, 2017; revision accepted Jan. 9, 2018.

For correspondence or reprints contact: Hendrik Rathke, Department of Nuclear Medicine, University Hospital Heidelberg, INF 400, 69120 Heidelberg, Germany.

E-mail: hendrik.rathke@med.uni-heidelberg.de

Published online Jan. 25, 2018.

contrast, the value of PSMA imaging in patients with advanced-stage disease has not been evaluated systematically. With the recent introduction of PSMA radioligand therapy, the interest in this field is increasing. Targeting therapies can be effective only if the target is sufficiently expressed in most tumor lesions. Therefore, all available studies of ^{177}Lu- or ^{225}Ac-PSMA ligand therapy have been performed on patients preselected by PSMA imaging (*18–20*). However, the highest possible resolution (i.e., that obtained with PET) might not be necessary in this setting, and ^{99m}Tc-based PSMA ligands might represent a clinical alternative. In this medical situation, patients scheduled for PSMA-targeting therapy at our clinic receive both conventional BS and PSMA-targeting ^{99m}Tc-MIP-1427 scintigraphy within a short interval.

The aim of this retrospective analysis was to compare BS with ^{99m}Tc-methylene diphosphonate (^{99m}Tc-MDP) and PSMA ligand ^{99m}Tc-MIP-1427 in patients with known osseous metastasized prostate cancer.

MATERIALS AND METHODS

Patients

Twenty-one patients who had metastatic castration-resistant prostate cancer and were preparing for possible PSMA radioligand therapy underwent both conventional BS including SPECT and PSMA SPECT/CT for staging. For all patients, the examinations were performed within 10 d of each other (mean and median, 7 d). Table 1 shows the characteristics of the patients.

Selection criteria for this retrospective evaluation were the availability of PSMA and BS performed on the basis of clinical indications within 10 d. The examinations were conducted in accordance with the Helsinki Declaration ("unproven intervention in clinical practice") and national regulations [German Pharmaceutical Products Act, AMG §13(2b)]. All patients signed a written informed consent form. The ethical committee of the University Hospital Heidelberg approved this retrospective evaluation.

Radiopharmaceuticals

The PSMA ligand MIP-1427 was labeled with ^{99m}Tc as already described (*21*). The precursor was produced in-house as previously described (*22*) and labeled in accordance with the described protocol but with a minor modification: the deprotected precursor was radiolabeled with the tricarbonyl method using a conventional IsoLink kit (Covidien). Quality control for ^{99m}Tc-labeled PSMA ligand MIP-1427 was performed by reversed-phase high-performance liquid chromatography, and ^{99m}Tc-labeled PSMA ligand MIP-1427 was discarded if purity was lower than 95%. Quality control for ^{99m}Tc-MDP BS was performed by chromatography in accordance with the manufacturer's (ROTOP-MDP) requirements for purity.

Application and Imaging Protocol

The ^{99m}Tc-MDP solution was applied via an intravenous catheter as a bolus injection of 693 ± 33 (mean ± SD) MBq. ^{99m}Tc-MIP-1427 was also applied intravenously as a bolus injection (672 ± 94 MBq) via a sterile filter system (Filtropur S 0.2; Sarstedt). Clinical conditions during application and imaging were observed to detect possible adverse events.

For BS, images were acquired 2 h after injection. Planar images were acquired with an ECAM scanner system (Siemens), and SPECT imaging (Infinia Hawkeye 4 scanner system; GE Healthcare) included 2 fields of view of 40 cm per bed position. The first field of view covered the neck/thorax, and the second field of view covered the abdomen/pelvis. PSMA imaging was performed 3 h after nuclide application. Imaging included planar scintigraphy with the ECAM scanner and 2-field-of-view SPECT/CT with the Infinia Hawkeye 4 scanner, covering the neck/thorax and the abdomen/pelvis.

TABLE 1
Patient Characteristics

Patient characteristic	Value*
Age (y)	
Median	75.5
Range	57–85
Gleason score	
Median	8
No. of patients with Gleason score of:	
<7	2
7	6
8	2
9	6
Unknown	5
PSA (ng/mL)	
Median	502
Range	6–1,855
Alkaline phosphatase (U/L)	
Mean	166.8
SD	121.8
Localization of metastases	
Lymph node(s)	9
Bone	21
Liver	1
Lung	5
Brain	1
Other	2
Local recurrence	1
Previous therapy	
RPx	10
LRTx	13
CRPC	21
Abiraterone (Zytiga; Janssen Biotech, Inc.)	17
Enzalutamide (Xtandi; Astellas Pharma Inc.)	12
Zoledronic acid (Zometa; Novartis)/denosumab (Xgeva; Amgen Inc.)	8
$^{223}RaCl_2$ (Xofigo; Bayer)	9
CTx	13

*Values are reported as numbers of patients unless otherwise indicated.

RPx = radical prostatectomy; LRTx = local radiation therapy; CRPC = castration-resistant prostate cancer; CTx = chemotherapy.

For planar images acquired with the ECAM scanner, low-energy high-resolution collimators were used. The scan velocity was 15 cm/min in a 1,025 × 256 matrix. For SPECT imaging acquired for BS and PSMA scanning, the Infinia Hawkeye 4 scanner system was used with low-energy high-resolution collimation and the following parameters: 128 × 128 matrix; zoom of 1; step-by-step scan by 30 s and 120 images with a 3° angle cut in a 128 × 128 matrix. CT imaging for attenuation correction and lesion evaluation was performed as 4-slice low-dose CT in the Infinia

Hawkeye 4 scanner system (140 keV; 40 mAs) on the same day as the PSMA scan and included the neck/thorax and abdomen/pelvis regions.

To reduce the radiation dose, as there is no clinical indication for 2 CT scans in this setting within 10 d, only PSMA imaging was amended by SPECT/CT, whereas BS was amended by SPECT. Afterward, the CT data from PSMA SPECT/CT were transferred to a Siemens Leonardo workstation (*syngo* MultiModality Workplace VE36A), and software fusion to the bone SPECT data was performed using an automatic soft-fusion toolkit.

Masked Reading

The intensity of tumor uptake was scored visually. Planar images of PSMA scans and ^{99m}Tc-MDP bone scans were anonymized and masked for image assessment by 5 nuclear medicine physicians (3 with >5 y of experience and 2 residents in their third and fourth years). Lesions in planar scans were interpreted with regard to their respective characteristic patterns: normal, equivocal, or tumor pattern. Lesion locations were grouped for further analysis; predefined regions were scalp, sternum, thorax, shoulder/scapula, upper arm, lower arm, upper spine, middle spine, lower spine, sacroiliac joint, hip, thighs, knees, and lower limbs. Figure 1 shows further details. In a second step, SPECT for BS (including the CT dataset [soft fusion]) and SPECT/CT (hybrid imaging) for PSMA scanning were unmasked, and the findings were reevaluated, taking into account the additional information.

Consensus Reading

Consensus reading was performed after the evaluation of planar imaging and SPECT/CT (soft fusion for bone; hybrid imaging for PSMA) and was amended with all other available clinical information and with data that were acquired from imaging modalities (such as CT, MRI, and PET) during the follow-up period. The results were evaluated by the 5 observers against the definition of the gold standard. This concept (best evaluable comparator) was applied previously in other radiologic research (*23*). For each patient, a clinical follow-up of at least 6 mo (or until death) was available. Future imaging modalities were chosen according to the respective clinical needs and were not bound to a specific protocol. The ongoing evaluation of primary unknown or equivocal findings usually led to a definite result, as lesions disappeared, remained at a constant level, or grew rapidly (characteristic for malignant lesions in this patient collective with short PSA doubling times).

Statistical Analysis

For every anatomic region and patient, we determined whether each of the readers agreed with the consensus result, in regard to both the 2–step evaluation (benign or malignant) and the finer, 5-step evaluation (normal, equivocal [probably benign], equivocal [probably malignant], focal tumor, or diffuse tumor). The average number (± SD) of readers agreeing with the consensus reading was determined for each method and each patient, and the results were compared using a 2-sided Wilcoxon signed rank test. The results were assessed using Microsoft Excel 2007 (Microsoft Corp.) and R Version 3.3.2 (R Foundation for Statistical Computing). The statistical significance level was set at a P value of less than or equal to 0.05.

Sensitivity and specificity for both PSMA scanning and BS were calculated separately for each reader and region and then averaged, first over readers and then over regions. SEs were calculated for each estimate. Differences between methods were checked for significance using 2-sided paired t tests.

RESULTS

No adverse events during application and imaging were reported. All images of ^{99m}Tc-MDP scans (n = 21) and PSMA scans (n = 21) were evaluable. In 3 patients, equal findings from BS and PSMA scanning were present. In 16 patients, PSMA scanning identified more suspect lesions than BS. In 4 patients, ^{99m}Tc-MDP–negative but PSMA-positive bone marrow involvement was present. In 3 patients, more bone lesions were detected with PSMA scanning than with BS.

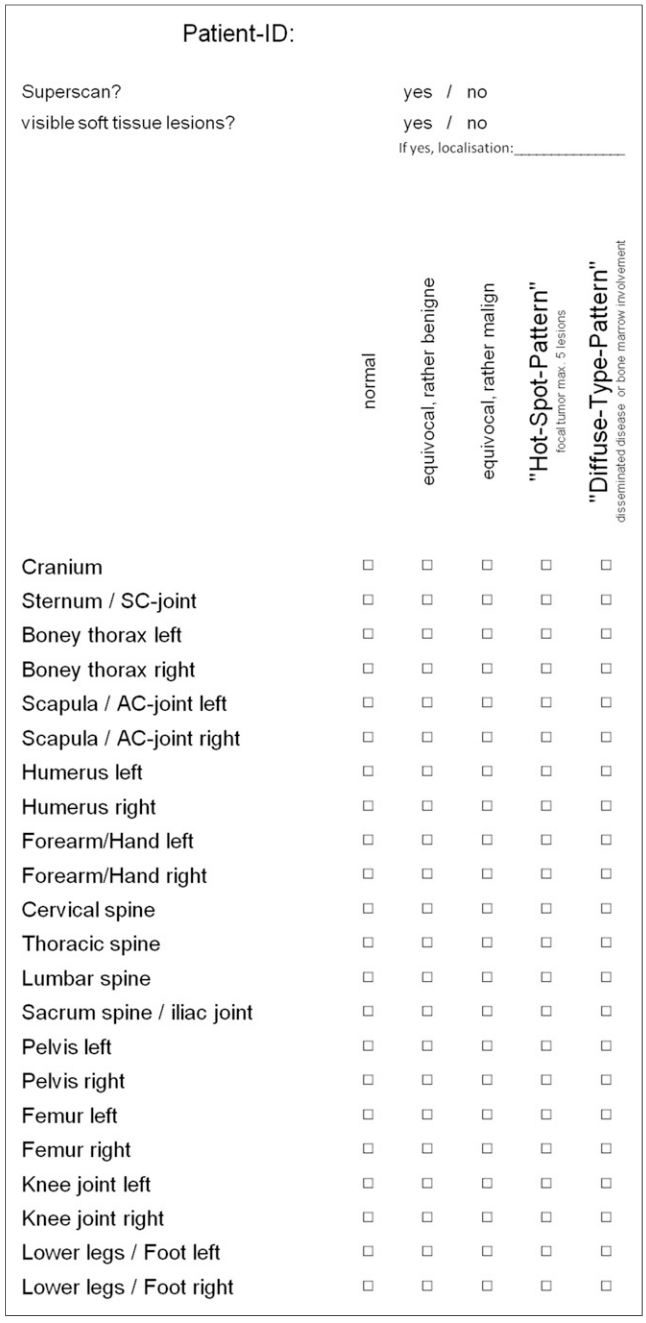
Patient-ID:

Superscan? yes / no

visible soft tissue lesions? yes / no

If yes, localisation:_____

	normal	equivocal, rather benigne	equivocal, rather malign	"Hot-Spot-Pattern" focal tumor max. 5 lesions	"Diffuse-Type-Pattern" disseminated disease or bone marrow involvement
Cranium	☐	☐	☐	☐	☐
Sternum / SC-joint	☐	☐	☐	☐	☐
Boney thorax left	☐	☐	☐	☐	☐
Boney thorax right	☐	☐	☐	☐	☐
Scapula / AC-joint left	☐	☐	☐	☐	☐
Scapula / AC-joint right	☐	☐	☐	☐	☐
Humerus left	☐	☐	☐	☐	☐
Humerus right	☐	☐	☐	☐	☐
Forearm/Hand left	☐	☐	☐	☐	☐
Forearm/Hand right	☐	☐	☐	☐	☐
Cervical spine	☐	☐	☐	☐	☐
Thoracic spine	☐	☐	☐	☐	☐
Lumbar spine	☐	☐	☐	☐	☐
Sacrum spine / iliac joint	☐	☐	☐	☐	☐
Pelvis left	☐	☐	☐	☐	☐
Pelvis right	☐	☐	☐	☐	☐
Femur left	☐	☐	☐	☐	☐
Femur right	☐	☐	☐	☐	☐
Knee joint left	☐	☐	☐	☐	☐
Knee joint right	☐	☐	☐	☐	☐
Lower legs / Foot left	☐	☐	☐	☐	☐
Lower legs / Foot right	☐	☐	☐	☐	☐

FIGURE 1. Report form for standardized evaluation of masked patients.

Agreement of Raters

The ratio of typical benign and probably benign lesions and the ratio of typical malignant and probably malignant lesions are shown in Table 2.

TABLE 2
Ratio of Equivocal to Normal or Malignant Lesions

Type of lesion	Tracer	Description of lesion	No. of findings	Ratio
Benign	^{99m}Tc-MDP	Normal	687	1.9:1
		Equivocal	366	
	PSMA	Normal	858	27.7:1
		Equivocal	31	
Malignant	^{99m}Tc-MDP	Malignant	1,049	4.9:1
		Equivocal	214	
	PSMA	Malignant	1,271	8.1:1
		Equivocal	156	

The agreement of raters with the consensus reading was significantly greater for PSMA scanning than for ^{99m}Tc-MDP BS (Table 3). On the 2-step scale (benign or malignant), 0.43 ± 0.36 of 5 misclassifications were observed for PSMA and 0.76 ± 0.64 of 5 misclassifications were observed for ^{99m}Tc-MDP ($P = 0.039$). On the 5-step scale (normal, equivocal benign, equivocal malignant, focal tumor, or diffuse tumor), an average of 1.45 ± 0.39 of 5 raters misclassified each region using PSMA scans and an average of 2.41 ± 0.66 of 5 raters misclassified each region using ^{99m}Tc-MDP scans ($P < 0.001$). The results for senior physicians and residents were comparable.

Sensitivity/Specificity

A significant difference ($P < 0.001$) was detected between the 92% sensitivity of PSMA scanning (SE = 2%) and the 76% sensitivity of ^{99m}Tc-MDP BS (SE = 3%) for the evaluation of bone lesions. On planar scans, the specificity of PSMA scanning for bone lesions was 86% (SE = 3%) and that of ^{99m}Tc-MDP BS was 90% (SE = 2%). Differences in specificity were not significant ($P = 0.13$).

After unmasking of the additional SPECT/CT data, the test quality criteria for ^{99m}Tc-MDP remained unchanged. However, the specificity of PSMA for patients with phenotype-positive cancers improved from 86% to 97% (significant). The data for 1 patient with a PSMA-negative but ^{99m}Tc-MDP–positive tumor phenotype are shown in Figure 2. The main reason for the low specificity of planar PSMA scans was liver and lung metastases that were projected on ribs and consequently scored as false-positive bone metastases on 2-dimensional planar scans. These dislocations were successfully allocated using transverse slices (Fig. 3).

TABLE 3
Agreement of Raters with Consensus Reading

	2-Step evaluation		5-Step evaluation	
Parameter	PSMA	^{99m}Tc-MDP	PSMA	^{99m}Tc-MDP
Median	0.36	0.55	1.55	2.23
Mean	0.43	0.76	1.45	2.41
Misclassification rate	9%	15%	29%	48%
SD	0.39	0.66	0.36	0.64
P	0.039		<0.001	

In 2-step evaluation, only correspondence according to benign vs. malignant was evaluated. In 5-step evaluation, correct alignment of normal, equivocal benign, equivocal malignant, focal tumor, and diffuse tumor in comparison to consensus reading was evaluated. Mean indicates average number of misclassifications out of 5 raters. Misclassification rate indicates portion of raters with misclassification vs. consensus reading of mean.

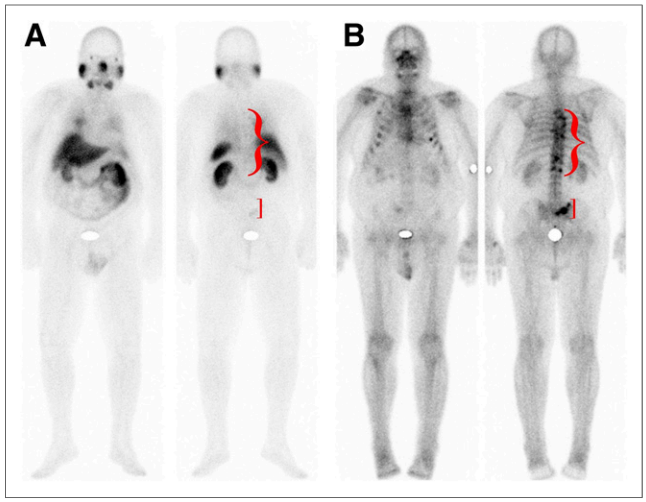

FIGURE 2. Patient with PSMA-negative tumor phenotype. No pathologic findings in spine or pelvis were depicted with PSMA (A) but were successfully diagnosed by BS (B).

In 11 of 21 patients, lymphadenopathy or soft-tissue lesions were present in addition to bone lesions. For the 2 patients with PSMA-negative tumors, no visceral metastases or growing lymph nodes were reported during the follow-up period, and calculation of test quality criteria (such as sensitivity or specificity) was not reasonable. For the 19 patients with a PSMA-positive tumor phenotype, correlations with the whole set of clinical data (including other imaging modalities, such as MRI) (Fig. 4) and follow-up examinations were added to the consensus reading. PSMA-positive soft-tissue lesions did not show any false-positive findings. Heterogeneous PSMA expression and bone turnover in BS were present in 1 patient and led to various interpretations (Fig. 5); no gold standard could be defined for this patient during the consensus reading, but follow-up data implied that PSMA-positive and PSMA-negative lesions could occur within 1 patient.

Tumor lesions in heavily burdened joints (e.g., knee and acromioclavicular joint) were more often misinterpreted as degenerative or equivocal lesions by ^{99m}Tc-MDP BS. After unmasking of morphologic imaging, these findings could successfully be verified; this sequence represents the actual clinical work flow. However, PSMA-positive or -negative findings in ^{99m}Tc-MIP-1427 scans were already correct without additional examinations. Figure 6 shows an example of a lesion that was interpreted as having a degenerative nature with ^{99m}Tc-MDP but as a typical tumor with ^{99m}Tc-MIP-1427.

Special Case: Superscan Pattern

Seven patients had a superscan pattern on ^{99m}Tc-MDP BS, and all skeletal regions were considered to show tumor involvement. For these patients, PSMA imaging allowed the delineation of specific lesions in the peripheral limbs (Fig. 7). The treating physicians interpreted the additional information regarding the extent of

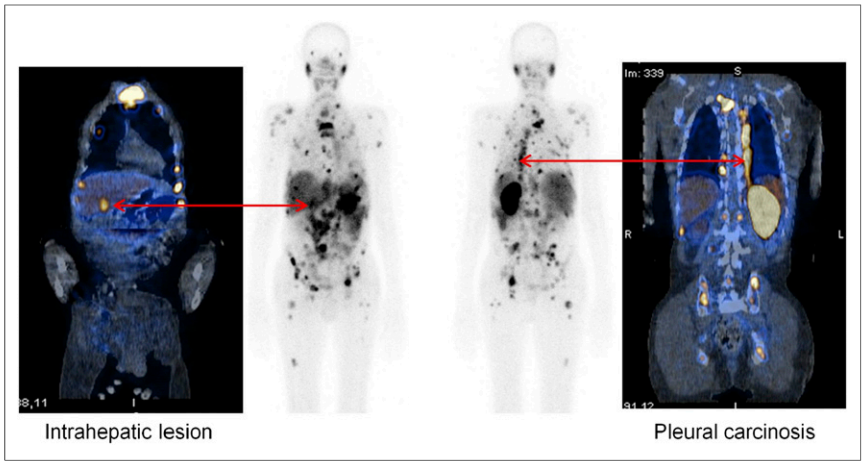

FIGURE 3. Intrahepatic lesion and pleural carcinosis. Three-dimensional imaging was pivotal for correct allocation of respective lesions. In particular, liver and lung lesions were often misinterpreted and falsely assigned to overlapping bone structures.

red marrow involvement as helpful for estimating the red marrow reserve before initiating the next therapeutic treatment line instead of best supportive care. Improvements in clinical decisions for these patients were not assessed in this analysis.

DISCUSSION

The imaging findings for ^{99m}Tc-PSMA scanning and BS were evaluated in patients who had known bone metastases and were scheduled for an evaluation of PSMA-targeting therapy, which requires PSMA imaging in advance. With regard to this objective, PSMA scans were sufficient to determine whether patients had PSMA-positive or -negative tumor phenotypes.

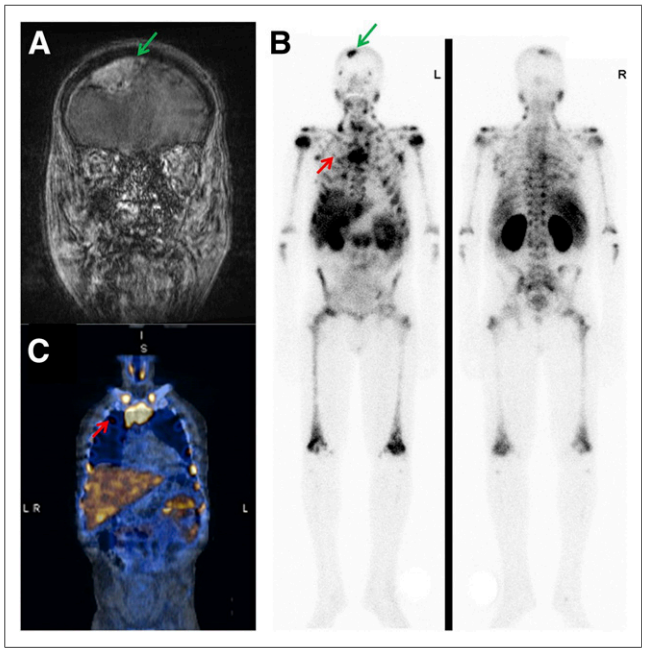

FIGURE 4. Patient with intracerebral metastasis (A, green arrow) that was misinterpreted as skull lesion on planar scan (B, green arrow). Similarly, pulmonary lesion (C, red arrow) was also misinterpreted as rib lesion (B, red arrow). (A) MRI. (B) ^{99m}Tc-PSMA whole-body scan. (C) ^{99m}Tc-PSMA SPECT/CT.

Other groups have already reported comparisons between ^{68}Ga-PSMA PET/CT and planar BS with (*24*) or without (*25,26*) routinely performed SPECT. These reports had some remarkable limitations; for example, the mean intervals between the imaging modalities were 21 d (range not reported) (*25*), up to 80 d (*24*), or up to 100 d (*26*). One advantage of our analysis was that both imaging procedures were performed within a median of 7 d (maximum, 10 d). However, this strict patient selection criterion was responsible for the smaller number of evaluable patients in our analysis—a limitation of our evaluation. Another limitation of the previous reports was the comparison of scintigraphy and PET. An advantage for the imaging modality with the higher inherent resolution and the better signal-to-noise ratio was predictable. Several researchers have already found an advantage of ^{18}F-fluoride PET over multi–field-of-view SPECT/CT and planar ^{99m}Tc BS (*11,13,27,28*). Thus, for the comparison of PSMA PET/CT and ^{18}F-fluoride PET/CT, only case reports are available (*29,30*). To our knowledge, our data represent the first comparison of ^{99m}Tc-PSMA imaging and ^{99m}Tc BS using the same imaging modality and parameters.

With regard to diagnostic performance, we found several advantages for the PSMA scan, at least for PSMA-positive tumors, which are present in most metastatic castration-resistant prostate cancer patients. Evaluation of the agreement of raters with the consensus reading indicated less reader-dependent influence on PSMA scanning than on ^{99m}Tc-MDP BS. PSMA imaging commonly reported typical benign or typical malignant lesions, showing a decrease in equivocal findings and a decrease in misclassifications of tumor spread (Table 2). The probability for equivocal findings decreased by using PSMA imaging. For example, benign lesions were found with a normal-to-equivocal ratio of

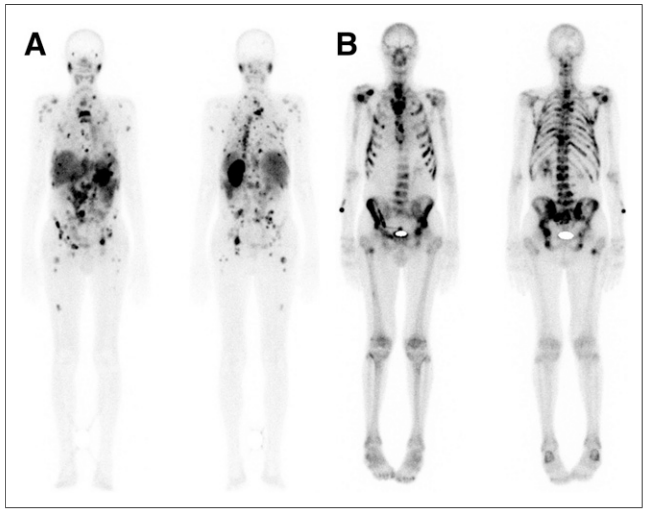

FIGURE 5. In patient with heterogeneously PSMA-expressing lesions, PSMA scanning (A) presented highly discordant lesion distribution pattern in comparison to ^{99m}Tc-MDP BS (B).

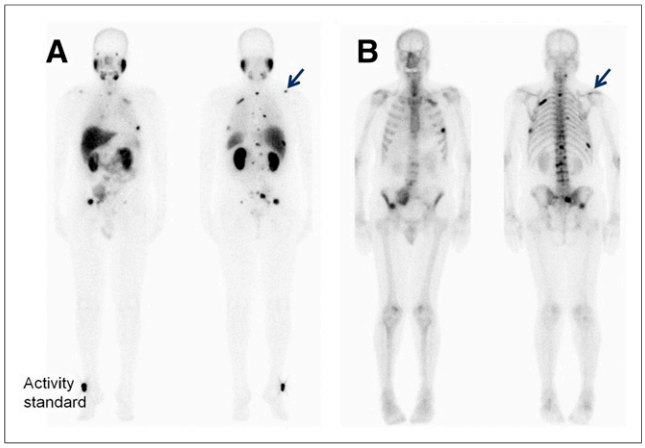

FIGURE 6. PSMA imaging (A, arrow) of typical malignant lesion that was scored as equivocal by BS (B, arrow).

27.7:1 for PSMA and only 1.9:1 for MDP scanning (Table 2). On the basis of our results, every third lesion detected with ^{99m}Tc-MDP BS remained unclear. In current practice, equivocal findings require further evaluation with additional imaging of higher specificity, such as MRI focused on a particular lesion (*23*). Thus, the widespread use of PSMA scintigraphy may be useful for reducing additional examinations.

Our data suggested a relatively high sensitivity of PSMA imaging (92%) in comparison to ^{99m}Tc-MDP imaging (76% [BS]) for planar scans. These data are concordant with previously published data, although those were from intermodal comparisons of SPECT or SPECT/CT and PET/CT (*26*). Pyka et al. calculated sensitivities of 98.7%–100% for PET/CT (*26*).

For planar imaging, the specificity of 86% for PSMA was lower but not significantly different from that of 90% for BS. However, when ^{99m}Tc-based PSMA imaging was conducted and evaluated as SPECT/CT, the accuracy of our results was close to that of PSMA PET/CT. These results showed that the planar imaging technique was not optimal for correct tumor allocation. Especially for non–organ-confined tumor tracers, the improvement of hybrid imaging was highly pronounced. A benefit of SPECT/CT over planar BS was also reported previously (*11,13,27,28*). In contrast to these literature data, we did not observe a significant improvement of SPECT/CT (soft fusion) over planar images for BS. Therefore, a possible explanation is the high prevalence of true-positive bone metastases in comparison to only a few equivocal degenerative lesions in our cohort with advanced-stage disease.

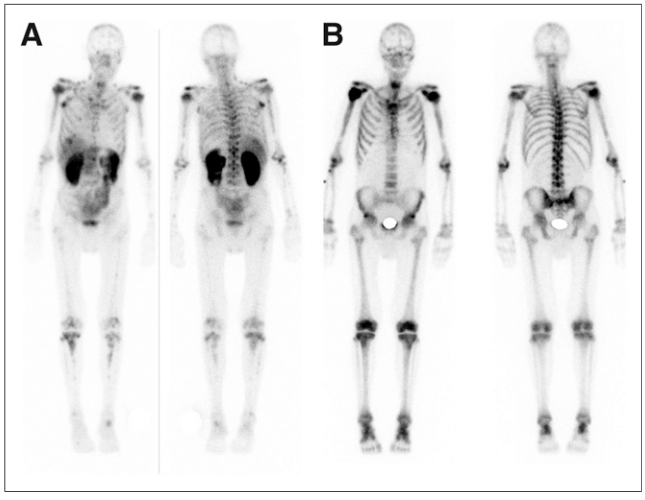

FIGURE 7. Example of superscan pattern in patient imaged by PSMA scanning (A) and BS (B). Excessive tumor uptake in highly perfused red marrow resulted in at least relatively or even absolutely reduced uptake in salivary glands (PSMA scanning) and kidneys (BS).

In our group of patients with late-stage disease, visceral metastases—such as those in the liver, lung, and brain—were common. In addition to bone lesions, soft-tissue lesions were present in 11 of 21 patients. In patients with advanced-stage disease, it seems mandatory for PSMA imaging to be performed as SPECT/CT, covering the complete field of view, to cope with the challenge of correct lesion allocation to overlapping organs. In contrast, early-stage prostate cancer has a low probability for visceral metastases; SPECT/CT focused on the pelvis may be sufficient to identify and allocate lymph node metastases, whereas planar whole-body scans can be used to rule out distant metastases (*14*). The diagnosis of visceral metastases is important for prognosis and treatment stratification, as visceral metastases or lymph nodes of greater than 3 cm prohibit the application of $^{223}RaCl_2$ and necessitate another therapeutic strategy (*31*).

In our retrospective patient population, 2 patients had insufficient PSMA uptake in lesions that were considered undoubtedly malignant in the reference examinations and follow-up. In these 2 patients, a weak or nonexistent PSMA-positive tumor phenotype may have been present. This finding is consistent with previously published data for PSMA-negative tumor sites in patients with biochemical relapse, irrespective of the PSA level (*1,32*). The demonstration of intense PSMA expression led to PSMA radioligand therapy. In contrast faint PSMA uptake, but intense uptake in BS, led to the decision that PSMA radioligand therapy was contraindicated. In such cases, a therapeutic regimen using bone-seeking drugs, such as ^{153}Sm-EDTMP or $^{223}RaCl_2$, may be more appropriate.

Because our patient collective was a cohort with very advanced disease and high pretest probability, true-positive and, consequently, highly specific findings were present disproportionately. In contrast, the similar sensitivity and specificity found with PSMA PET/CT were derived from patients with clinically more challenging conditions. The specificity of SPECT imaging in our cohort with a high tumor burden seems to be overestimated, especially because recently published data indicated the superiority of ^{68}Ga-PSMA PET/CT over ^{99m}Tc-PSMA SPECT/CT, particularly in patients with low-volume disease or PSA relapse (*33,34*).

CONCLUSION

In this intraindividual comparison of PSMA scans and bone scans, the PSMA tracer presented a clear advantage in most patients. The amount of equivocal findings decreased for PSMA scans in comparison to bone scans. However, SPECT or SPECT/CT was pivotal for differentiating between bone metastases and extraosseous tumor lesions.

DISCLOSURE

^{99m}Tc-MIP-1427 was synthesized and used for compassionate-use applications with the permission of Molecular Insight Pharmaceuticals, Inc. (subsidiary of Progenics Pharmaceuticals, Inc.). There was no funding or other support from either Molecular

Insight Pharmaceuticals, Inc., or Progenics Pharmaceuticals, Inc. Thomas Armor is a full-time employee of Progenics Pharmaceuticals, Inc. No other potential conflict of interest relevant to this article was reported.

REFERENCES

1. Afshar-Oromieh A, Holland-Letz T, Giesel FL, et al. Diagnostic performance of ^{68}Ga-PSMA-11 (HBED-CC) PET/CT in patients with recurrent prostate cancer: evaluation in 1007 patients. *Eur J Nucl Med Mol Imaging.* 2017;44:1258–1268.
2. Giesel FL, Sterzing F, Schlemmer HP, et al. Intra-individual comparison of ^{68}Ga-PSMA-11-PET/CT and multi-parametric MR for imaging of primary prostate cancer. *Eur J Nucl Med Mol Imaging.* 2016;43:1400–1406.
3. van Leeuwen PJ, Emmett L, Ho B, et al. Prospective evaluation of ^{68}gallium-prostate-specific membrane antigen positron emission tomography/computed tomography for preoperative lymph node staging in prostate cancer. *BJU Int.* 2017;119:209–215.
4. Goffin KE, Joniau S, Tenke P, et al. Phase 2 study of ^{99m}Tc-trofolastat SPECT/CT to identify and localize prostate cancer in intermediate- and high-risk patients undergoing radical prostatectomy and extended pelvic LN dissection. *J Nucl Med.* 2017;58:1408–1413.
5. Vallabhajosula S, Nikolopoulou A, Babich JW, et al. ^{99m}Tc-labeled small-molecule inhibitors of prostate-specific membrane antigen: pharmacokinetics and biodistribution studies in healthy subjects and patients with metastatic prostate cancer. *J Nucl Med.* 2014;55:1791–1798.
6. Barrett JA, Coleman RE, Goldsmith SJ, et al. First-in-man evaluation of 2 high-affinity PSMA-avid small molecules for imaging prostate cancer. *J Nucl Med.* 2013;54:380–387.
7. Reinfelder J, Kuwert T, Beck M, et al. First experience with SPECT/CT using a ^{99m}Tc-labeled inhibitor for prostate-specific membrane antigen in patients with biochemical recurrence of prostate cancer. *Clin Nucl Med.* 2017;42:26–33.
8. Cher ML, Bianco FJ Jr, Lam JS, et al. Limited role of radionuclide bone scintigraphy in patients with prostate specific antigen elevations after radical prostatectomy. *J Urol.* 1998;160:1387–1391.
9. Kane CJ, Amling CL, Johnstone PA, et al. Limited value of bone scintigraphy and computed tomography in assessing biochemical failure after radical prostatectomy. *Urology.* 2003;61:607–611.
10. Lipton A. Implications of bone metastases and the benefits of bone-targeted therapy. *Semin Oncol.* 2010;37(suppl. 2):S15–S29.
11. Even-Sapir E, Metser U, Mishani E, Lievshitz G, Lerman H, Leibovitch I. The detection of bone metastases in patients with high-risk prostate cancer: ^{99m}Tc-MDP planar bone scintigraphy, single- and multi-field-of-view SPECT, ^{18}F-fluoride PET, and ^{18}F-fluoride PET/CT. *J Nucl Med.* 2006;47:287–297.
12. Schirrmeister H, Guhlmann A, Elsner K, et al. Sensitivity in detecting osseous lesions depends on anatomic localization: planar bone scintigraphy versus ^{18}F PET. *J Nucl Med.* 1999;40:1623–1629.
13. Abikhzer G, Srour S, Fried G, et al. Prospective comparison of whole-body bone SPECT and sodium ^{18}F-fluoride PET in the detection of bone metastases from breast cancer. *Nucl Med Commun.* 2016;37:1160–1168.
14. Scher HI, Morris MJ, Stadler WM, et al. Trial design and objectives for castration-resistant prostate cancer: updated recommendations from the Prostate Cancer Clinical Trials Working Group 3. *J Clin Oncol.* 2016;34:1402–1418.
15. Heidenreich A, Bastian PJ, Bellmunt J, et al. EAU guidelines on prostate cancer. Part 1: screening, diagnosis, and local treatment with curative intent—update 2013. *Eur Urol.* 2014;65:124–137.
16. Heidenreich A, Bastian PJ, Bellmunt J, et al. EAU guidelines on prostate cancer. Part II: treatment of advanced, relapsing, and castration-resistant prostate cancer. *Eur Urol.* 2014;65:467–479.
17. Cornford P, Bellmunt J, Bolla M, et al. EAU-ESTRO-SIOG guidelines on prostate cancer. Part II: treatment of relapsing, metastatic, and castration-resistant prostate cancer. *Eur Urol.* 2017;71:630–642.
18. Kratochwil C, Bruchertseifer F, Rathke H, et al. Targeted alpha-therapy of metastatic castration-resistant prostate cancer with ^{225}Ac-PSMA-617: dosimetry estimate and empiric dose finding. *J Nucl Med.* 2017;58:1624–1631.
19. Rahbar K, Ahmadzadehfar H, Kratochwil C, et al. German multicenter study investigating ^{177}Lu-PSMA-617 radioligand therapy in advanced prostate cancer patients. *J Nucl Med.* 2017;58:85–90.
20. Heck MM, Retz M, D'Alessandria C, et al. Systemic radioligand therapy with ^{177}Lu labeled prostate specific membrane antigen ligand for imaging and therapy in patients with metastatic castration resistant prostate cancer. *J Urol.* 2016;196:382–391.
21. Hillier SM, Maresca KP, Lu G, et al. ^{99m}Tc-labeled small-molecule inhibitors of prostate-specific membrane antigen for molecular imaging of prostate cancer. *J Nucl Med.* 2013;54:1369–1376.
22. Lu G, Maresca KP, Hillier SM, et al. Synthesis and SAR of ^{99m}Tc/Re-labeled small molecule prostate specific membrane antigen inhibitors with novel polar chelates. *Bioorg Med Chem Lett.* 2013;23:1557–1563.
23. Lecouvet FE, El Mouedden J, Collette L, et al. Can whole-body magnetic resonance imaging with diffusion-weighted imaging replace Tc 99m bone scanning and computed tomography for single-step detection of metastases in patients with high-risk prostate cancer? *Eur Urol.* 2012;62:68–75.
24. Janssen JC, Meissner S, Woythal N, et al. Comparison of hybrid ^{68}Ga-PSMA-PET/CT and ^{99m}Tc-DPD-SPECT/CT for the detection of bone metastases in prostate cancer patients: additional value of morphologic information from low dose CT. *Eur Radiol.* 2018;28:610–619.
25. Thomas L, Balmus C, Ahmadzadehfar H, Essler M, Strunk H, Bundschuh RA. Assessment of bone metastases in patients with prostate cancer: a comparison between ^{99m}Tc-bone-scintigraphy and [^{68}Ga]Ga-PSMA PET/CT. *Pharmaceuticals (Basel).* 2017;10:E68.
26. Pyka T, Okamoto S, Dahlbender M, et al. Comparison of bone scintigraphy and ^{68}Ga-PSMA PET for skeletal staging in prostate cancer. *Eur J Nucl Med Mol Imaging.* 2016;43:2114–2121.
27. Abikhzer G, Gourevich K, Kagna O, Israel O, Frenkel A, Keidar Z. Whole-body bone SPECT in breast cancer patients: the future bone scan protocol? *Nucl Med Commun.* 2016;37:247–253.
28. Langsteger W, Rezaee A, Pirich C, Beheshti M. ^{18}F-NaF-PET/CT and ^{99m}Tc-MDP bone scintigraphy in the detection of bone metastases in prostate cancer. *Semin Nucl Med.* 2016;46:491–501.
29. Uprimny C, Kroiss A, Nilica B, et al. ^{68}Ga-PSMA ligand PET versus ^{18}F-NaF PET: evaluation of response to ^{223}Ra therapy in a prostate cancer patient. *Eur J Nucl Med Mol Imaging.* 2015;42:362–363.
30. Rowe SP, Mana-Ay M, Javadi MS, et al. PSMA-based detection of prostate cancer bone lesions with ^{18}F-DCFPyL PET/CT: a sensitive alternative to ^{99m}Tc-MDP bone scan and Na^{18}F PET/CT? *Clin Genitourin Cancer.* 2016;14:e115–e118.
31. Parker C, Nilsson S, Heinrich D, et al. Alpha emitter radium-223 and survival in metastatic prostate cancer. *N Engl J Med.* 2013;369:213–223.
32. Afshar-Oromieh A, Avtzi E, Giesel FL, et al. The diagnostic value of PET/CT imaging with the ^{68}Ga-labelled PSMA ligand HBED-CC in the diagnosis of recurrent prostate cancer. *Eur J Nucl Med Mol Imaging.* 2015;42:197–209.
33. Schmidkonz C, Hollweg C, Beck M, et al. ^{99m}Tc-MIP-1404-SPECT/CT for the detection of PSMA-positive lesions in 225 patients with biochemical recurrence of prostate cancer. *Prostate.* 2018;78:54–63.
34. Lawal IO, Ankrah AO, Mokgoro NP, Vorster M, Maes A, Sathekge MM. Diagnostic sensitivity of Tc-99m HYNIC PSMA SPECT/CT in prostate carcinoma: a comparative analysis with Ga-68 PSMA PET/CT. *Prostate.* 2017;77:1205–1212.